Available online at www.sciencedirect.com
SCIENCE DIRECT
Carbohydrate Research 341 (2006) 610–615
Carbohydrate RESEARCH

Metal–ion interactions with carbohydrates. Crystal structure and FT-IR study of the $SmCl_3$–ribose complex

Yan Lu[a,*] and Jianyu Guo[b]

[a]*Department of Chemical Engineering, Shanghai Institute of Technology, Shanghai 200235, China*
[b]*Department of Chemistry, Shanghai Normal University, Shanghai 200234, China*

Received 16 October 2005; received in revised form 18 November 2005; accepted 21 November 2005
Available online 17 January 2006

Abstract—A single-crystal of $SmCl_3{\cdot}C_5H_{10}O_5{\cdot}5H_2O$ was obtained from methanol–water solution and its structure determined by X-ray. Two forms of the complex as a pair of anomers and related conformers were found in the single-crystal in a disordered state. One ligand is α-D-ribopyranose in the $^4C_1$ conformation and the other one is β-D-ribopyranose. The anomeric ratio is 1:1. Both ligands provide three hydroxyl groups in ax–eq–ax orientation for coordination. The Sm^{3+} ion is nine-coordinated with five Sm–O bonds from water molecules, three Sm–O bonds from hydroxyl groups of the D-ribopyranose and one Sm–Cl bond. The hydroxyl groups, water molecules and chloride ions form an extensive hydrogen-bond network. The IR spectral C–C, O–H, C–O, and C–O–H vibrations were observed to be shifted in the complex and the IR results are in accord with those of X-ray diffraction.

Keywords: Sm–D-ribose complex; Isomers; Crystal structure; FT-IR

1. Introduction

Saccharides are widely distributed in the bodies of animals, plants and microorganisms, and are considered as the third most important biomolecules after proteins and nucleic acids.[1] The multiple oxygen donor atoms in sugar molecules and the fact that metal cations co-exist in biological fluids suggest coordination between saccharides and metal ions may happen in living organisms and such reactions may have some particular biological relevance. A good example is the formation of Ni^{2+}–carbohydrate complex demonstrated in human kidney in 1985.[2] Recent researches have shown that such interactions have fundamental importance in many biochemical processes, such as the transfer and storage of metal ions,[3,4] the action of metal-containing pharmaceuticals, toxic-metal metabolism,[5,2] and Ca^{2+} mediated carbohydrate–protein binding.[6,7] Therefore, studies with regard to the metal ion binding properties of carbohydrates are of particular significance and should aid in understanding metal ion action during biological processes.

Information regarding the interactions of saccharides with metal cations is rather limited in the literature, especially for well-characterized solid complexes. Most previous work concerning metal–carbohydrate complexes is focused on their aqueous solution chemistry, and relatively few well-characterized solid complexes have been reported, especially for those sugars containing only alcoholic oxygen donor atoms. Up to the present, only the following neutral sugar–metal complexes have been determined by X-ray diffraction. They are the complexes of Mo^{6+}–D-xylose,[8] Ca^{2+}–D-fructose,[9–11] Ca^{2+}–D-galactose,[12] Ca^{2+}–lactose,[13,14] Na^+–sucrose,[15,16] Na^+–cellobiose,[17] Ca^{2+}–D-mannose,[18] Ca^{2+}–trehalose,[19] Ca^{2+}–D-xylose,[20] Ca^{2+}–L-arabinose,[21] Pr^{3+}–D-ribose,[22,23] Nd^{3+}–D-ribose,[24,25] Ca^{2+}–D-ribose,[26] $LaCl_3{\cdot}$ribose$\cdot 5H_2O$, and $CeCl_3{\cdot}$ribose$\cdot 5H_2O$.[27] The detailed three-dimensional structures of saccharides and the role of metal ions in determining and regulating these structures remain obscure.

* Corresponding author. E-mail: luuyann@vip.sina.com

0008-6215/$ - see front matter © 2005 Elsevier Ltd. All rights reserved.
doi:10.1016/j.carres.2005.11.018

D-Ribose ($C_5H_{10}O_5$), as a component of nucleic acids, exists in all organisms and is an important pentose. Accordingly, the metal–ion-binding properties may have some biological significance. Solution studies show that D-ribose exists in aqueous solution as an equilibrium mixture of mainly six isomers. Among the isomers, those having an ax–eq–ax sequence of three adjacent hydroxyl groups are readily coordinated with metal cations and form 1:1 complexes in hydrophilic solvents. It was reported that the 'complexing' isomers represent altogether 43% of the D-ribose isomers and these were proved to be merely less than those of talose.[28] The interactions of Ca^{2+}, Sr^{2+}, Ba^{2+}, La^{3+}, Ce^{3+}, Pr^{3+}, Nd^{3+}, Sm^{3+}, Eu^{3+}, Gd^{3+}, and Tb^{3+} with D-ribose in neutral solutions have been studied by NMR and calorimetric methods,[29–31] and the stability constants have been calculated ($<10\ M^{-1}$ in most cases). However, structures of most of these complexes are still undefined because solid complexes are difficult to obtain. Since the first report on the crystal structure of $PrCl_3{\cdot}C_5H_{10}O_5{\cdot}5H_2O$ in 2001, only five such ribose–metal complexes, from Ca^{2+}, La^{3+}, Ce^{3+}, Pr^{3+}, and Nd^{3+}, have so far been obtained as solids.

In the present work, a single-crystal of Sm^{3+} complex from D-ribose was obtained. Its crystal structure was determined by X-ray and compared with those that have been reported, and the vibration spectrum has been assigned and interpreted in correlation with the crystal structure.

2. Experimental

2.1. Materials

$SmCl_3$ was prepared from the corresponding rare earth oxide of high purity (99.99%).[32] D-Ribose was purchased from Acros and was used without further purification.

2.2. Preparation of $SmCl_3{\cdot}C_5H_{10}O_5{\cdot}5H_2O$

D-Ribose (0.45 g, 3 mmol) and equivalent amounts of $SmCl_3$ were dissolved in water–MeOH, and the solution was evaporated slowly until crystallization occurred. Anal. Calcd for $SmCl_3{\cdot}C_5H_{10}O_5{\cdot}5H_2O$: C, 12.08; H, 4.03. Found: C, 12.04; H, 4.05.

2.3. Physical measurements

The mid-IR spectrum was measured on a Nicolet Magna-IR 750 spectrometer using the micro-IR method, 128 scans at $4\ cm^{-1}$ resolution.

The structure of $SmCl_3{\cdot}C_5H_{10}O_5{\cdot}5H_2O$ was determined on a Bruker Smart 1000 diffractometer using monochromatic Mo Kα radiation ($\lambda = 0.71073$ Å) in the θ range from 2.08° to 26.37° at 293 K. The final cycle of full-matrix least-squares refinement was based on 2792 observed reflections. Calculations were completed with the SHELX-97 program.

Crystallographic data (without structure factors) for the structure reported in this paper have been deposited with the Cambridge Crystallographic Data Centre as supplementary publication No. CCDC-199654. Copies of the data can be obtained free of charge on application to the CCDC, 12 Union Road, Cambridge CB2 1EZ, UK. [Fax: (internat.) +44 1223/336033; e-mail: deposit@ccdc.cam.ac.uk.]

3. Results and discussion

3.1. X-ray crystal structures

In contrast to the single pyranose form observed, two anomeric configurations were observed in the single-crystal of $SmCl_3{\cdot}ribose{\cdot}5H_2O$ obtained by our group.

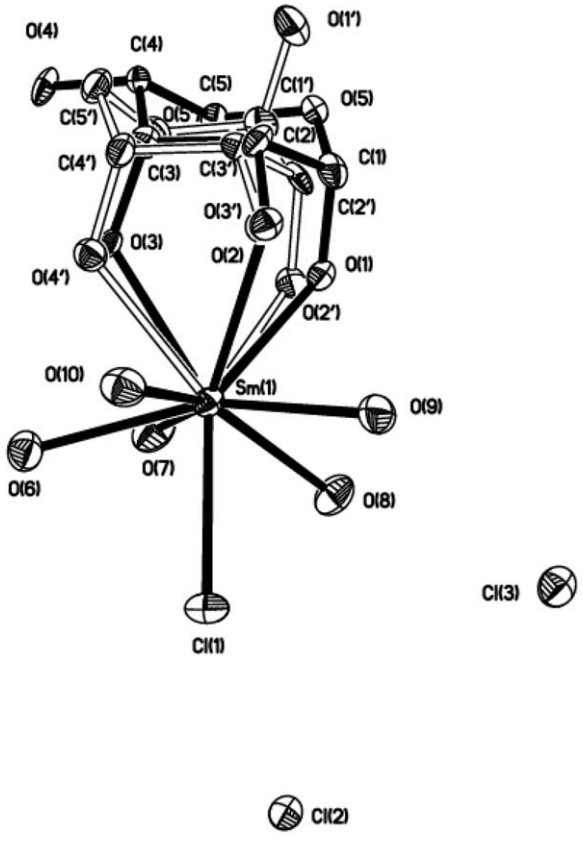

Figure 1. The structure and atom numbering scheme of $SmCl_3{\cdot}C_5H_{10}O_5{\cdot}5H_2O$. The ligand of the complex is in a disordered state, which indicates that there are two sets of $SmCl_3{\cdot}C_5H_{10}O_5{\cdot}5H_2O$ molecules in the single crystal. The one shown by solid bonds is α-D-ribopyranose in the $^4C_1$ conformation, and the other shown by open bonds is β-D-ribopyranose in the $^1C_4$ conformation (labeled by numbers with dashes).

The single-crystal of the title complex is disordered with two configurations forming a pair of anomers, and the structures are similar to those of $PrCl_3$·ribose·$5H_2O$, $NdCl_3$·ribose·$5H_2O$, $LaCl_3$·$C_5H_{10}O_5$·$5H_2O$, and $CeCl_3$·$C_5H_{10}O_5$·$5H_2O$ reported by our group.[23,25,27] The two structures of the title complex are shown together in Figure 1. Figure 2 shows the crystal unit cell of $SmCl_3$·β-ribopyranose·$5H_2O$ with β-ribopyranose in $^1C_4$ conformation. The crystal data and structure refinements of the complex are listed in Table 1.

Figure 1 shows that there are two kinds of $SmCl_3$·ribose·$5H_2O$ molecules with different anomeric configurations in the single crystal. The ribose moiety of one of the molecules is α-pyranose in the $^4C_1$ conformation (shown by solid bonds in Fig. 1). In the other $SmCl_3$·ribose·$5H_2O$ molecule, the ribose moiety is β-pyranose in the $^1C_4$ conformation (shown by open bonds in Fig. 1 and the atoms labeled by numbers with dashes). The α:β anomeric ratio is 1:1. In both of the $SmCl_3$·ribose·$5H_2O$ molecules, the Sm ion is nine-coordinated and binds to three hydroxyl groups of one D-ribopyranose molecule, five water molecules, and a chloride ion. The other two Cl^- ions in the molecule are 'free'. The three adjacent hydroxyl groups labeled O(1)H,O(2)H and O(3)H (in the α-ribopyranose $^4C_1$ conformation) or O(2′)H,O(3′)H and O(4′)H (in the β-ribopyranose $^1C_4$ conformation) which contains the ax–eq–ax sequence, are the coordination sites of the ribose. The ring oxygen of D-ribose does not coordinate with Sm^{3+} in either of the molecule. All water molecules in the crystal are coordinated in the two structures. The coordination behavior of La^{3+}, Ce^{3+}, Pr^{3+}, Nd^{3+}, and Sm^{3+} are shown to be similar from the X-ray results.

An extensive network of hydrogen bonds involving all hydroxyl groups, water molecules and chloride ions in the crystal of $SmCl_3$·$C_5H_{10}O_5$·$5H_2O$ was determined in this work, and the data are given in Table 2. The Sm–ribose complex molecules are organized by these hydrogen bonds and thus form layers parallel to the (10−1) plane. These layers are then also held together by hydrogen bonds with regular spaces between them (see Fig. 3). Free Cl ions distributed in these layers are responsible for not only the formation of a layer but also the bonding between the layers by hydrogen bonds. In the $SmCl_3$·$C_5H_{10}O_5$·$5H_2O$ complex, the Cl^- ions play important roles not only as counterions but

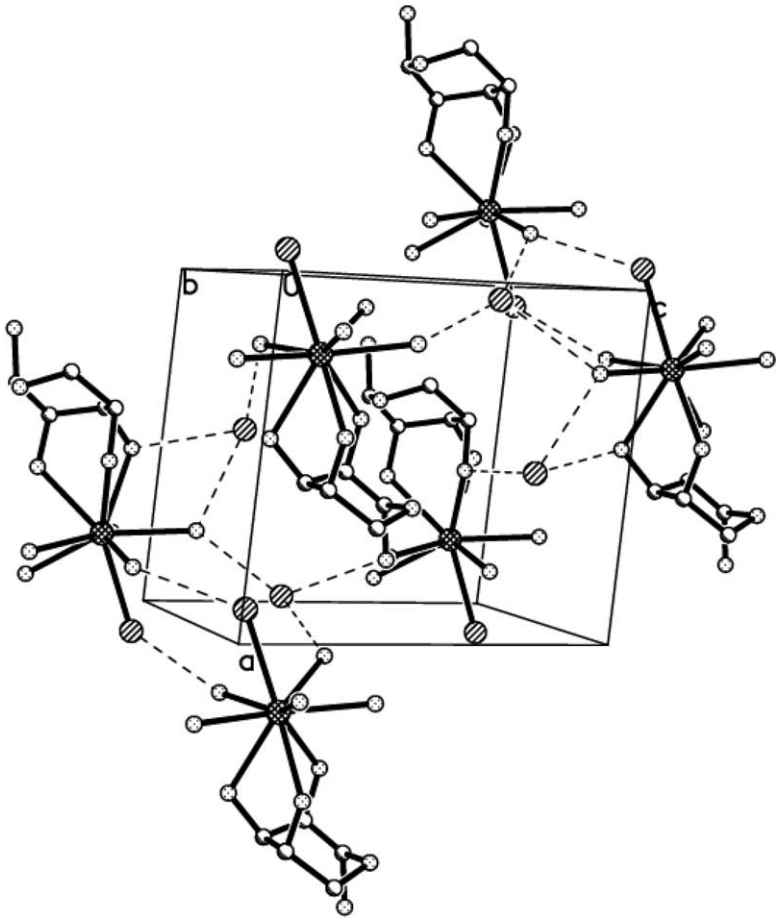

Figure 2. Projection of the crystal cell in the structure of $SmCl_3$·$C_5H_{10}O_5$·$5H_2O$. The ligand shown is β-D-ribopyranose in the $^1C_4$ configuration. The meaning of the balls in this figure are shown as follows: ▨ represents Cl, ● represents Sm, ⊗ represents O, ○ represents C.

Table 1. Crystal data and structure refinement parameters for $SmCl_3{\cdot}C_5H_{10}O_5{\cdot}5H_2O$

Formula	$SmCl_3{\cdot}C_5H_{10}O_5{\cdot}5H_2O$
Formula weight	496.91
Crystal system, Space group	Monoclinic, $P2(1)$
a (Å)	9.121(5)
b (Å)	8.814(5)
c (Å)	9.830(5)
β (°)	94.156(7)
V (Å^3)	788.2(7)
Z	2
D_{calcd} (Mg/m^3)	2.094
Absorption coefficient (mm^{-1})	4.270
$F(000)$	486
Crystal size (mm)	$0.25 \times 0.20 \times 0.20$
θ Range for data collection (°)	2.08–26.37
Index ranges	$-6 \leqslant h \leqslant 11$, $-10 \leqslant k \leqslant 10$, $-10 \leqslant l \leqslant 12$
Reflections collected/ unique	3582/2792 [R(int) = 0.0222]
Completeness to $\theta = 26.37$ (%)	98.3
Absorption correction	Semi-empirical from equivalents
Max/min transmission	0.4822 and 0.4149
Refinement method	Full-matrix least-squares on F^2
S	1.019
Final R indices [$I > 2\sigma(I)$]	$R1 = 0.0321$, $wR2 = 0.0678$
R indices (all data)	$R1 = 0.0422$, $wR2 = 0.0710$
Absolute structure parameter	0.07(2)
Largest difference peak and hole (e/Å^3)	1.303 and −0.711
Data/restraints/parameters	2792/0/265

Table 2. Hydrogen bonds for $SmCl_3{\cdot}C_5H_{10}O_5{\cdot}5H_2O$ with H···A < $r(A)$ + 2.000 Å and <DHA, >110°

D–H···A	d(D–H)	d(H···A)	d(D···A)	<(DHA)
O6–H6A···Cl3 #1	0.838	2.547	3.204	136.01
O6–H6B···Cl2 #2	0.843	2.675	3.477	159.58
O7–H7B···O5 #3	0.838	2.054	2.868	163.80
O7–H7B···O1′ #3	0.838	2.098	2.710	129.55
O8–H8A···Cl3	0.837	2.387	3.219	173.04
O8–H8B···O4 #4	0.838	2.312	3.031	144.15
O8–H8B···Cl3 #2	0.838	2.814	3.492	139.25
O9–H9A···Cl1 #5	0.839	2.431	3.173	147.78
O9–H9B···Cl2 #6	0.838	2.357	3.190	172.49
O10–H10A···Cl3 #7	0.844	2.659	3.260	129.33
O10–H10A···Cl1	0.844	2.814	3.204	110.20
O10–H10B···Cl2 #8	0.844	2.304	3.102	157.93
O1–H1···O4 #4	0.930	1.769	2.679	165.52
O2–H2···Cl2 #8	0.930	2.435	2.983	117.70
O3–H3···Cl2 #2	0.930	2.494	3.171	129.85
O4–H4···Cl3 #9	0.820	2.403	3.174	156.91
O1′–H1′···O8 #10	0.820	2.654	3.117	117.39
O2′–H2′···O5′ #4	0.930	2.330	2.914	120.47
O3′–H3′···Cl2 #8	0.930	2.611	3.104	113.66
O4′–H4′···Cl2 #2	0.930	2.094	2.914	146.33

Symmetry transformations used to generate equivalent atoms: (#1) x, $y-1$, z; (#2) $-x+$;1, $y-1/2$, $-z+1$; (#3) $-x$, $y-1/2$, $-z+1$; (#4) $-x$, $y+1/2$, $-z+1$; (#5) $-x+1$, $y+1/2$, $-z+2$; (#6) $-x+1$, $y+1/2$, $-z+1$ (#7) $-x+1$, $y-1/2$, $-z+2$; (#8) $x-1$, y, $z+1$; (#9) $x-1$, $y-1$, z; (#10) $x-1$, y, z.

also as the predominant feature in the network of hydrogen bonds.

3.2. IR spectroscopy study of Sm–ribose complex

The IR data of a series of metal–ribose complexes that were obtained by our group have been measured. For comparison, the absorption bands and tentative assignments of D-ribose and its complexes (La–ribose, Ce–ribose, Pr–ribose, Nd–ribose, and Sm–ribose complexes) are shown together in Table 3. The IR data of La–, Ce–, Pr–, Nd–, and Sm–ribose complexes including those reported by Yang et al. are similar, indicating that La^{3+}, Ce^{3+}, Pr^{3+}, Nd^{3+}, and Sm^{3+} have similar coordination mode.

The broad absorption band at around 3400 cm^{-1} in the spectrum of D-ribose can be assigned to the hydrogen-bonded OH groups. This band appears broader in the spectra of its metal complexes. The observed spectral changes are due to the metalation of the sugar and the rearrangement of the strong hydrogen-bonding network observed in the crystal structures of the complexes. The C–H stretching vibration bands in the spectrum of the title complex (2946, 2852, 2672, and 2538 cm^{-1}), corresponding to the band of 2928 cm^{-1} in the spectrum of free D-ribose, are observed weaker and masked by the broadened νOH bands. The band at about 1622 cm^{-1} in the spectrum of the complex can be assigned to the δ_{HOH} vibration of the coordinated water. The bands at 1452, 1417, 1340, and 1250 cm^{-1} in the spectrum of free D-ribose (see Table 3), which were assigned to the multiple bending vibrations of O–C–H, C–C–H, C–O–H, and CH_2, are observed to be shifted in the spectrum of the complex, and their intensities become weaker upon salt formation. The band at about 1150 cm^{-1} is the characteristic vibration of a pyranose form,[33] and it is observed in the spectrum of the title complex and D-ribose itself. In the 1200–970 cm^{-1} region, the C–O, C–C stretching vibrations and the C–O–H, C–C–O bending vibrations of D-ribose are observed to be shifted and split in the spectrum of the complex (see Table 3). Such observed splitting and shifting is indicative of the participation of the sugar hydroxyl groups in metal–ligand bonding, which therefore affects the C–O, C–C stretching vibrations and the C–O–H, C–C–O bending vibrations of the sugar moiety.

The ring skeletal deformation bands (δC–C–O and δC–C–C) of free D-ribose, mainly in the 1000–400 cm^{-1} region, show considerable changes on complex formation (see Table 3). This may be attributed to distortion of the sugar ring upon metalation. However, no crystal data for free D-ribose have been reported to permit comparison with those of the complex. The spectral changes observed in this region may be interpreted

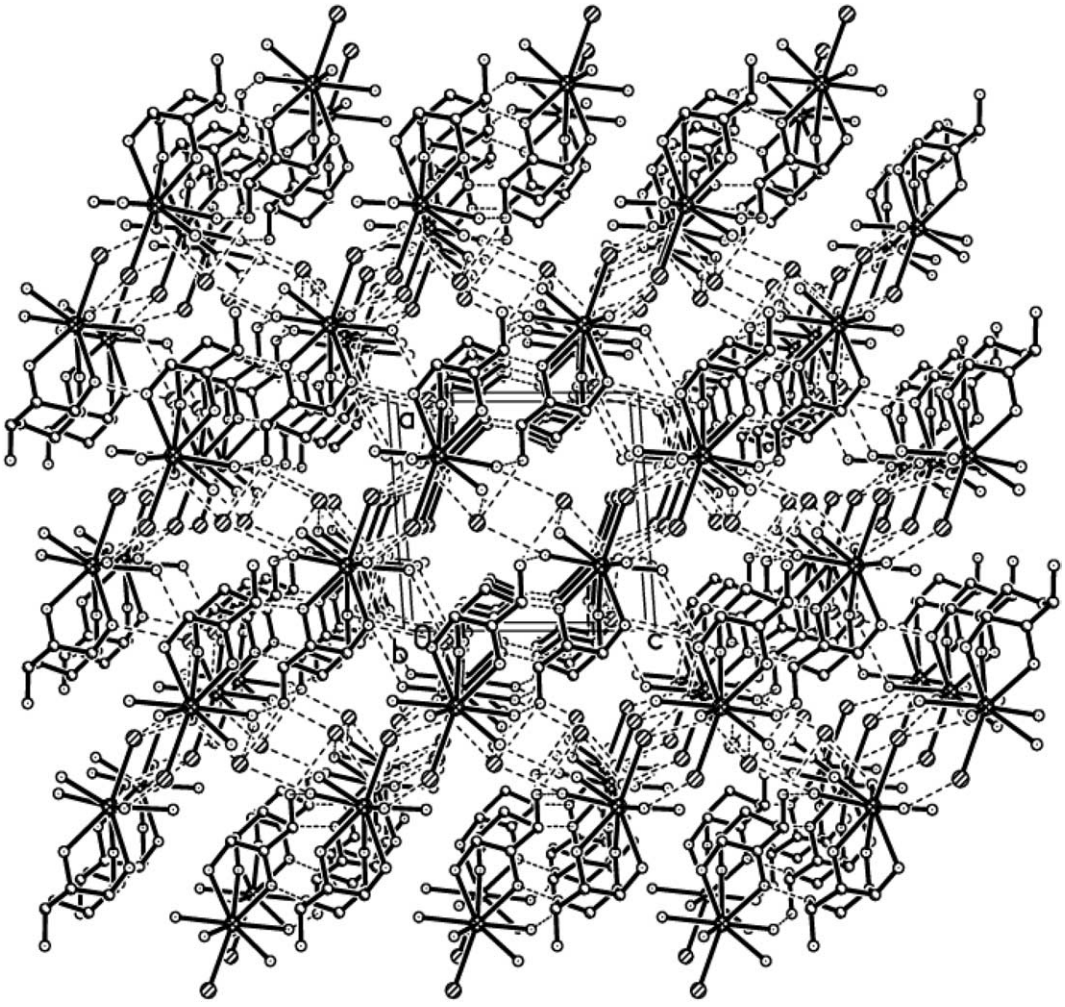

Figure 3. Projection of the packed crystal in the structure of $SmCl_3{\cdot}C_5H_{10}O_5{\cdot}5H_2O$ along the *b*-axis. (The meaning of the balls in this figure are same as those in Fig. 2.)

Table 3. IR data for D-ribose, La–ribose, Ce–ribose, Pr–ribose, Nd–ribose and Sm–ribose complexes (1500–700 cm^{-1})

D-Ribose	La–ribose[27]	Ce–ribose[27]	Pr–ribose[22]	Nd–ribose[25]	Sm–ribose	Possible assignment[33–38]
1452	1457	1458	1458	1456	1458	δOCH + δCCH + δCH_2
1417	1410	1417	1409	1408	1407	δOCH + δCCH
1340	1348	1348	1350	1350	1350	δOCH + δCCH + δCOH
	1319	1318	1318	1315	1317	δOCH + δCCH + δCOH
1250	1244	1244	1244	1244	1244	δCCH + δCOH + δOCH
1153	1152	1153	1152	1153	1151	νC–O + νC–C + δCOH(pyranose)
1117	1128	1127	1128	1128	1128	νC–O + νC–C + δCOH
1085	1093	1094	1095	1091	1094	νC–O + νC–C + δCOH
1042	1047	1047	1048	1047	1048	νC–O + νC–C + δCCO
	1004	1004	1004	1003	1004	νC–O + νC–C + δCCO
987	971	971	972	971	972	νC–O + νC–C + δCCO
914	917	917	918	918	917	νC–O + δCCH + ν asy(ring of pyranose)
887	885	886	887	888	887	νC–O + νC–C + δCCH
872	874	874	874	874	874	δCH(β-pyranose)
	835	835	836	836	836	δCH(α-pyranose)
826						δCH
795	793	794	795	796	798	τC–O + δCCO + δCCH + ν sy(ring of pyranose)
746	734	735	736	734	738	τC–O + δCCO + δCCH

δ, bending mode; ν, stretching mode; and τ, twisting.

to indicate that metalation of the sugar perturbs the electron distribution within the sugar ring system, where the vibrations are mostly localized, and finally causes ring distortion, resulting in the alterations in the spectra. The 914 cm^{-1} and 795 cm^{-1} bands in the D-ribose spectrum are attributed to the asymmetric and symmetric ring-breathing modes of the pyranose. They are observed as bands at around 917 and 798 cm^{-1} in the Sm–ribose complex (see Table 3), indicating that the six-membered sugar ring is retained in the complex. The absorption bands at about 870 and 840 cm^{-1} in a pyranose spectrum are generally assigned to the presence of the β- and α-anomers, respectively.[34,35] In relation to the spectrum of the title complex, the coexistence of the absorption bands at about 874 and 836 cm^{-1} indicates that the complex is, in fact, a mixture with both α-ribopyranose and β-ribopyranose as ligands, and the two configurations of the complex indicated by the IR data are in accord with the X-ray results.

The IR results indicate that the hydroxyl groups of D-ribose take part in the metal–oxygen interaction; the hydrogen-bond network rearranges upon metalation; and there are two isomers coexisting in the complex with both α-ribopyranose and β-ribopyranose as ligands. The IR results are in accord with those of X-ray diffraction, and the FT-IR technique is thus a useful method for detecting the formation of such complexes.

References

1. Luo, J. S. *Biochemistry*; Huadong Normal University Press: Shanghai, 1997.
2. Templeton, D. M.; Sarkar, B. *Biochem. J.* **1985**, *230*, 35–42.
3. Sauchelli, V. *Trace Elements in Agriculture*; Van Nostrand: New York, 1969; p 248.
4. Holm, R. P.; Berg, J. M. *Pure Appl. Chem.* **1984**, *56*, 1645–1657.
5. Predki, P. F.; Whitfield, D. M.; Sarkar, B. *Biochem. J.* **1992**, *281*, 835–841.
6. Weis, W. I.; Drickamer, K.; Hendrickson, W. A. *Nature* **1992**, *360*, 127–134.
7. Drickamer, K. *Nature* **1992**, *360*, 183–186.
8. Taylor, G. E.; Waters, J. M. *Tetrahedron Lett.* **1981**, *22*, 1277–1278.
9. Craig, D. C.; Stephenson, N. C.; Stevens, J. D. *Cryst. Struct. Commun.* **1974**, *3*, 277–281.
10. Craig, D. C.; Stephenson, N. C.; Stevens, J. D. *Cryst. Struct. Commun.* **1974**, *3*, 195–199.
11. Cook, W. J.; Bugg, C. E. *Acta Crystallogr.* **1976**, *32*, 656–659.
12. Cook, W. J.; Bugg, C. E. *J. Am. Chem. Soc.* **1973**, *95*, 6442–6446.
13. Bugg, C. E. *J. Am. Chem. Soc.* **1973**, *95*, 908–913.
14. Cook, W. J.; Bugg, C. E. *Acta Crystallogr., Sect. B* **1973**, *29*, 907–909.
15. Accorsi, C. A.; Bellucci, F.; Bertolasi, V.; Ferretti, V. *Carbohydr. Res.* **1989**, *191*, 91–104.
16. Accorsi, C. A.; Bellucci, F.; Bertolasi, V.; Gilli, G. *Carbohydr. Res.* **1989**, *191*, 105–116.
17. Peralta-Inga, Z.; Johnson, G. P.; Dowd, M. K.; Rendleman, J. A.; Stevens, E. D.; French, A. D. *Carbohydr. Res.* **2002**, *337*, 851–861.
18. Craig, D. C.; Stephenson, N. C.; Stevens, J. D. *Carbohydr. Res.* **1972**, *22*, 494–495.
19. Cook, W. J.; Bugg, C. E. *Carbohydr. Res.* **1973**, *31*, 265–275.
20. Richards, G. F. *Carbohydr. Res.* **1973**, *26*, 448–449.
21. Terzis, A. *Cryst. Struct. Commun.* **1978**, *7*, 95–99.
22. Yang, L. M.; Zhao, Y.; Xu, Y. Z.; Jin, X. L. *Carbohydr. Res.* **2001**, *334*, 91–95.
23. Lu, Y.; Guo, J. Y. *Carbohydr. Res.*, in press.
24. Yang, L. M.; Wu, J. G.; Weng, S. F.; Jin, X. L. *J. Mol. Struct.* **2002**, *612*, 49–57.
25. Lu, Y.; Deng, G. C.; Miao, F. M.; Li, Z. M. *Carbohydr. Res.* **2003**, *338*, 2913–2919.
26. Lu, Y.; Deng, G. C.; Miao, F. M.; Li, Z. M. *J. Inorg. Biochem.* **2003**, *96*, 487–492.
27. Lu, Y.; Deng, G. C.; Miao, F. M.; Li, Z. M. *Carbohydr. Res.* **2004**, *339*, 1689–1696.
28. Angyal, S. J. *Pure Appl. Chem.* **1973**, *35*, 131–146.
29. Alvarez, A. M.; Desrosiers, N. M.; Morel, J. P. *Can. J. Chem.* **1987**, *65*, 2656–2660.
30. Desrosiers, N. M.; Lhermet, C.; Morel, J. P. *J. Chem. Soc., Faraday Trans.* **1991**, *87*, 2173–2177.
31. Desrosiers, N. M.; Lhermet, C.; Morel, J. P. *J. Chem. Soc., Faraday Trans.* **1993**, *89*, 1223–1228.
32. Chandrasekhar, A. *J. Imaging Technol.* **1990**, *16*, 158–161.
33. Cael, J. J.; Koenig, J. L.; Blackwell, J. *Carbohydr. Res.* **1974**, *32*, 79–91.
34. Tajmir-Riahi, A. H. *Carbohydr. Res.* **1983**, *122*, 241–248.
35. Tajmir-Riahi, A. H. *Carbohydr. Res.* **1984**, *127*, 1–8.
36. Zhang, W. J. *Biochemical Technology of Complexes of Carbohydrate*; Zhejiang University Press: Hangzhou, 1999; pp 193–198.
37. Mathlouthi, M.; Seuvre, A. M.; Koenig, J. L. *Carbohydr. Res.* **1983**, *122*, 31–47.
38. Tajmir-Riahi, A. H. *Biophys. Chem.* **1986**, *23*, 223–228.